

Spin-Polarized Electron Transport through Nanometer-Scale Al Grains

L. Y. Zhang, C. Y. Wang, Y. G. Wei, X. Y. Liu, and D. Davidović

Georgia Institute of Technology, Atlanta, GA 30332

(Dated: May 23, 2019)

Abstract

We investigate spin-polarized electron transport through ensembles of nanometer scale Al grains connected in parallel, at 4.2K. We demonstrate spin-valve effect and the Hanle effect. The tunnelling magnetoresistance (*TMR*) depends strongly on current direction, which we explain by comparing spin-coherence time T_2 and asymmetric electron dwell times. *TMR* decreases rapidly with bias voltage, suggesting that T_2 scales with electron-phonon energy-relaxation time, analogous to the Elliot-Yafet relation in bulk metals. This leads to an estimate $T_2 \approx 0.6 \text{ ms}$, which tells that quantum computation could be feasible at 4.2K.

Long spin relaxation times for polarized carriers are necessary for development of spintronic devices [1, 2, 3]. In quantum dots, spin relaxation times are strongly enhanced compared to bulk, and the spin of an electron confined in a quantum dot is a candidate quantum bit [4, 5]. At present, most measurements of spin-coherence times T_2 in semiconductors have used optical techniques and have shown that spin coherence time in bulk semiconductors can be quite long, of order ns [6].

On the other hand, the spin-flip time in a strong magnetic field (T_1) was measured by electron transport in semiconducting quantum dots [7, 8]. These measurements showed that T_1 can be extremely long, up to $\sim ms$. This suggests that T_2 might also be enhanced, because the maximum value of T_2 is $2T_1$ [9]. But, there is no guarantee that T_2 in quantum dots is greatly enhanced, because $T_2 \ll T_1$ in bulk.

Spin-injection and detection from ferromagnetic electron reservoirs is a proven technique to measure T_2 [10]. Effective electrical injection of spin polarized carriers into nonmagnetic semiconductors has proven to be difficult, possibly because of the conductivity mismatch between the metallic injecting electrodes and the semiconductor [11]. In metallic grains, however, the problem of inefficient spin-injection is bypassed.

In this paper we describe electron spin-injection (and detection) measurements in ensembles of Al-grains. Ensembles have the advantage that extremely long electron dwell times can be measured by standard electron transport. Long dwell times are necessary because they need to be comparable to T_2 , which is long.

Now we summarize the results of this paper. We show that electron-transport through the grains is spin-coherent in one current direction and spin-incoherent in the other current direction. This demonstrates that the dwell times are larger than T_2 . Spin-polarization of the current decreases rapidly with bias voltage, suggesting that T_2 scales with electron-phonon relaxation time. We apply the Elliot-Yafet equation [12] and find $T_2 \approx 0.6ms$ at 4.2K, which is extremely long. This suggests that quantum computing could be feasible at 4.2K, because long T_2 is one of the requirements for quantum computing. Finally, we present the effect of spin-precessions around the applied perpendicular field.

Our tunnelling device is sketched in Fig. 1-A. The top and the bottom layers are 100\AA thick Co films. The width/length is $1.5\text{mm}/15\text{mm}$ and $1\text{mm}/20\text{mm}$ for the bottom and the top layer, respectively.

The sample cross-section, sketched in Fig. 1-B, shows nanometer scale Al grains embedded

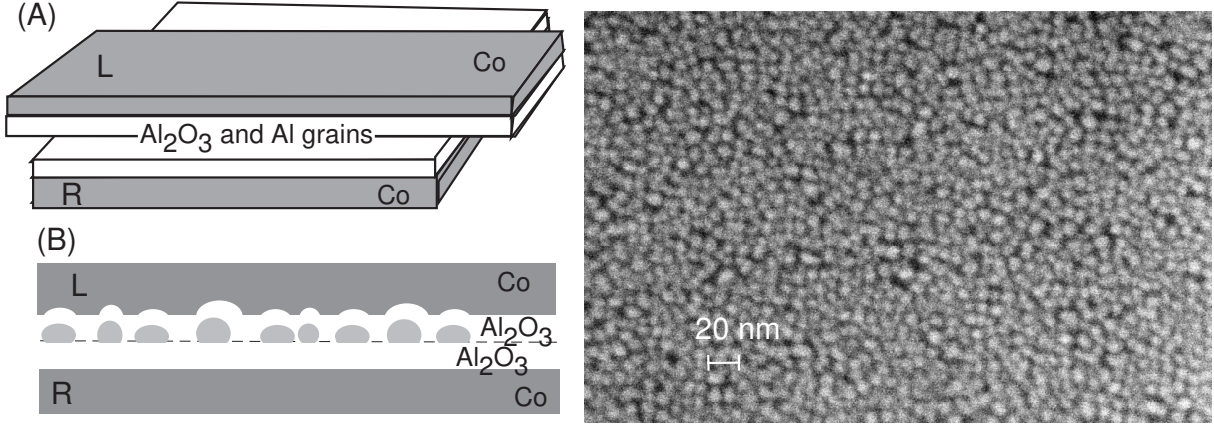


FIG. 1: A: Sketch of the tunnelling device geometry. B: Sketch of the tunnelling junction cross-section. C: Scanning electron micrograph of Al grains.

in Al_2O_3 . The device is a recreation of a tunnelling device made by Zeller and Giaver in the 1960s [13], which demonstrated Coulomb Blockade for the first time. The difference between our sample and the prior devices is that we have spin-polarized leads.

The device is fabricated in two evaporation steps. First, we thermally evaporate a Co film on a SiO_2 substrate, through a mask at $4 \cdot 10^{-7}$ Torr pressure. Next, we deposit 2\AA of Al at the same pressure. Then we introduce Oxygen at $3 \cdot 10^{-5}$ Torr for 30sec, to oxidize the Al-film. In the next step, we evaporate 50\AA of Al at this pressure at $2\text{\AA}/s$, which creates the first Al_2O_3 film.

The sample is now exposed to air and the mask is replaced. Next, the sample is evacuated to base pressure and we deposit $\sim 15\text{\AA}$ of Al, which creates isolated grains, as shown by the image in Fig. 1-C. Next, we deposit another layer of Al_2O_3 , using the same parameters as above. Finally, we deposit the top Co layer.

We assume that the grains have pancake shape. The average grain diameter is $\sim 12\text{\AA}$. Particle-in-a-box mean level spacing δ based on the diameter is $0.22meV$. The number of grains is $N = 2.5 \cdot 10^{10}$.

The resistances between the grains and the two leads are not uniformly distributed among grains. This is evidenced by the fact that the sample resistance R fluctuates among different samples in interval $1k\Omega < R < 1M\Omega$. Although these fluctuations may appear to be large, they can be explained by the fluctuations in the oxide thickness from grain to grain and the exponential dependence of the tunnelling resistance with the thickness. The number of

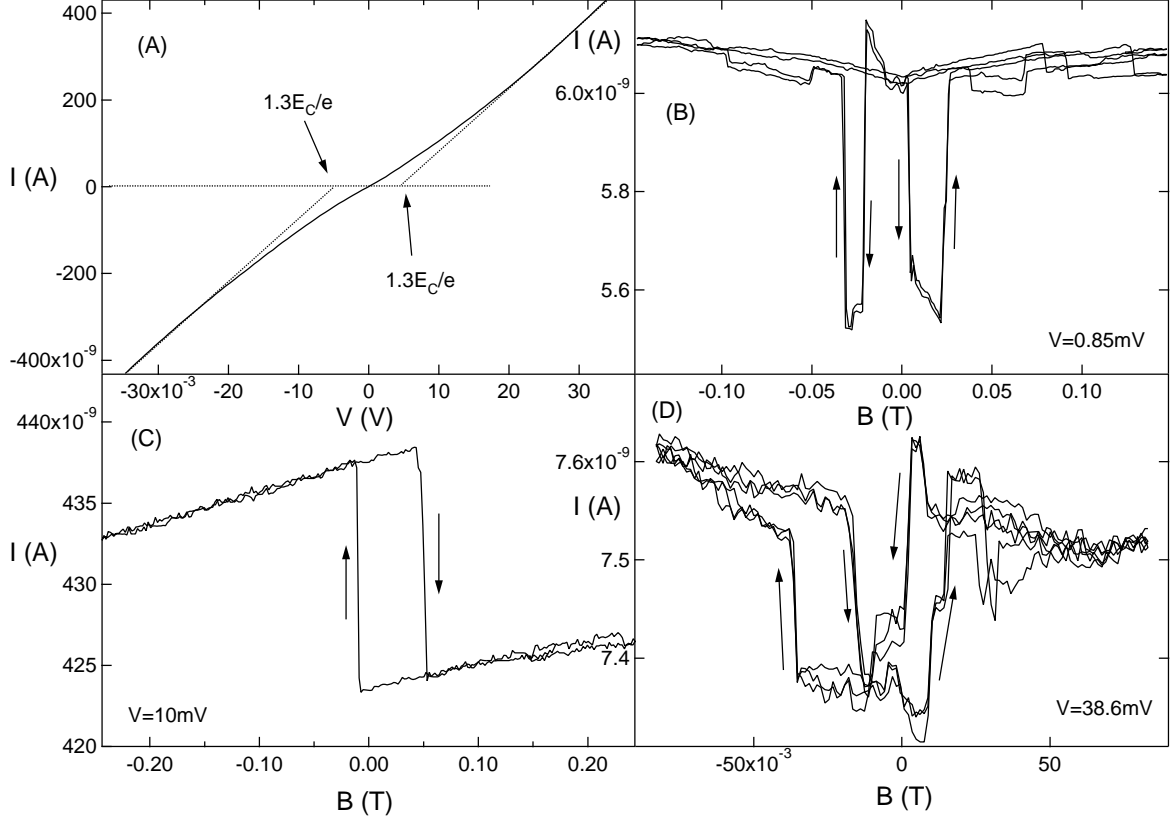


FIG. 2: A: IV-curves of sample 1 at 4.2K. B, C, and D: Current versus parallel applied magnetic field at 4.2K, in samples 1,2, and 3, respectively.

grains that contribute significantly to the conductance is $\ll N$.

We made tunnelling junctions as described above but without Al grains, and found that these devices were insulating. Thus, the leakage current between the leads is negligible.

In this paper we present three devices. Fig. 2-A displays the IV-curve of sample 1 at 4.2K. The other two samples have similar IV-curves. The conductance is suppressed at zero bias voltage, as expected from Coulomb-Blockade, consistent with Ref. [13].

The average charging energy E_C is obtained by extrapolating the linear part of the IV-curve at high V to zero I and finding the offset voltage, as indicated. We averaged the Coulomb Staircase IV-curve [14] over the background charge, capacitance ratios, and over capacitance range $(C/4, 7C/4)$, where C is the total capacitance of a grain. The corresponding offset was $1.3E_C/e$, where $E_C = e^2/2C$. E_C is $4.3meV$ in samples 1 and 2 and $6meV$ in sample 3. These values are larger than E_C in Ref. [15] for grains of comparable size, which

we explain by the larger oxide thickness in our devices.

Figs. 2-B,C, and D display current versus magnetic field in samples 1,2, and 3 respectively, at constant bias voltage. All samples exhibit TMR , which demonstrates that the tunnelling current is spin-polarized. Samples 1 and 3 exhibit a spin-valve effect: at a large negative field, the magnetizations of the reservoirs are down. If the field increases, the magnetization of one Cobalt film switches direction, and the tunnelling current drops discontinuously from $I_{\downarrow\downarrow}$ to $I_{\downarrow\uparrow}$. Finally, at a larger positive field the current jumps back up to $I_{\uparrow\uparrow} \approx I_{\downarrow\downarrow}$. In sample 2, only one jump is seen in this field range. At a much larger positive field (not shown), there is a smaller upward jump in the current. The tunnelling magnetoresistance is calculated as

$$TMR = (I_{\uparrow\uparrow} - I_{\downarrow\downarrow})/I_{\downarrow\downarrow}. \quad (1)$$

Figs. 3-A and B display differential conductance G with bias voltage in samples 1 and 2, respectively. G is measured by the lock-in technique. As the bias voltage is varied slowly at 3mv/hr, the magnetic field is swept between -0.25T and 0.25T at 0.01Hz. The differential conductance switches between $G_{\uparrow\uparrow}$ and $G_{\downarrow\downarrow}$ when the magnetizations switch alignment.

The dashed and the dotted line in Fig. 3-A is a guide to $G_{\downarrow\downarrow}$ and $G_{\uparrow\uparrow}$, respectively. The important information displayed here is that $G_{\uparrow\uparrow} - G_{\downarrow\downarrow}$ changes significantly when the bias voltage varies in a narrow interval around zero-bias voltage, i.e. the distance between the dashed and the dotted line changes around zero bias voltage. In sample 2, the asymmetry in $G_{\uparrow\uparrow} - G_{\downarrow\downarrow}$ is dramatic. The conductance is spin-unpolarized at negative bias and significantly spin-polarized at positive bias. That is, electron transport is spin polarized in one direction of transport and spin unpolarized in the opposite direction.

TMR also changes significantly around zero bias voltage, as shown in Fig. 3-C and D. Circles show TMR obtained directly from current using Eq. 1. Squares show TMR obtained from conductance using $TMR = \int G_{\uparrow\uparrow}(V)dV / \int G_{\downarrow\downarrow}(V)dV - 1$.

At low positive bias voltage, TMR is 0.08 and 0.12 in samples 1 and 2. To obtain spin-polarization in the leads, we first neglect spin relaxation in the grains and assume that spin polarized current arises from spin-dependent density of states in the reservoirs. The Julliere model [16] relates TMR and P as $TMR = 2P^2/(1 - P^2)$, where $P = (N_{\uparrow} - N_{\downarrow})/(N_{\uparrow} + N_{\downarrow})$ is the spin-polarization in the leads, and N_{\uparrow} and N_{\downarrow} are the spin-up and spin-down densities of states, respectively. It follows that $P = 0.2$ and $P = 0.24$ in samples 1 and 2, which is quite large, only a factor of 2 smaller than ideal P in Co. This demonstrates that spin-decoherence

cannot be strong at small positive bias.

The asymmetry in TMR with voltage has not been observed in conventional magnetic tunnelling junctions. In our tunnelling junctions, this effect can be explained by the asymmetry in electron dwell times. Assume the average resistance R_L between one reservoir (L) and the grains is much smaller than the average resistance R_R between the other reservoir and the grains, $R_L \ll R_R$. Asymmetric resistances are easily introduced by sample fabrication. For example, exposure of the bottom Al_2O_3 layer to air increases the Al_2O_3 thickness by hydration.

If a positive voltage is applied to lead L, then L will be an electron drain and the dwell time will be τ_L . If a negative voltage is applied to lead L, then L will be an electron source and the dwell time will be τ_R . Theoretically, $\tau_{L,R} \sim \frac{R_{L,R} \hbar}{R_Q \delta}$, where $R_Q = h/e^2 = 25k\Omega$. Consequently, the dwell time is much smaller at positive bias voltage.

TMR will be asymmetric if $T_2 < \tau_R$. For example, in sample 2, figure 3-B indicates that $\tau_L \sim T_2 \ll \tau_R$ ($\tau_L \sim T_2$ because P is large). The voltage interval around zero bias where the dwell times change is given by the Coulomb Blockade thermal width ($7k_B T/e$), in agreement with Fig. 3-A and B [20].

Next, we discuss the dependence of TMR on bias voltage. TMR is weakly dependent on V in intervals $0.5mV < V < 3mV$ and $-3mV < V < -0.5mV$. At $V \sim 3.5mV$, TMR begins to decrease with V , and at a characteristic voltage ($\sim 6mV$) TMR is significantly reduced. This dependence cannot be explained by the effect of energy dependence in the density of states of Co, because the characteristic voltage for this effect is $\sim 0.1V$ [17], much larger than $6mV$.

To explain this effect, we propose that T_2 decreases with V because electron-phonon relaxation time τ_{e-ph} decreases with V . Electron-phonon interaction causes spin-decoherence because of the spin-orbit interaction, in analogy with the behavior in bulk. In bulk metals, T_2 can be estimated from τ_{e-ph} by the Elliot-Yafet relation, $T_2 = \tau_{e-ph}/\alpha$, where α is the scattering ratio (10^{-4} in Al) [18].

The electron phonon relaxation time is [19]

$$\frac{1}{\tau_{e-ph}(\omega)} = \left(\frac{2}{3}E_F\right)^2 \frac{\omega^3 \tau \delta}{2\rho \hbar^4 v_s^5}, \quad (2)$$

where E_F is the Fermi energy (11.7 eV), ρ is the ion-mass density (2.7 g/cm³), v_s is the sound velocity (6420 m/s), ω is the excitation energy, and τ is the elastic scattering time.

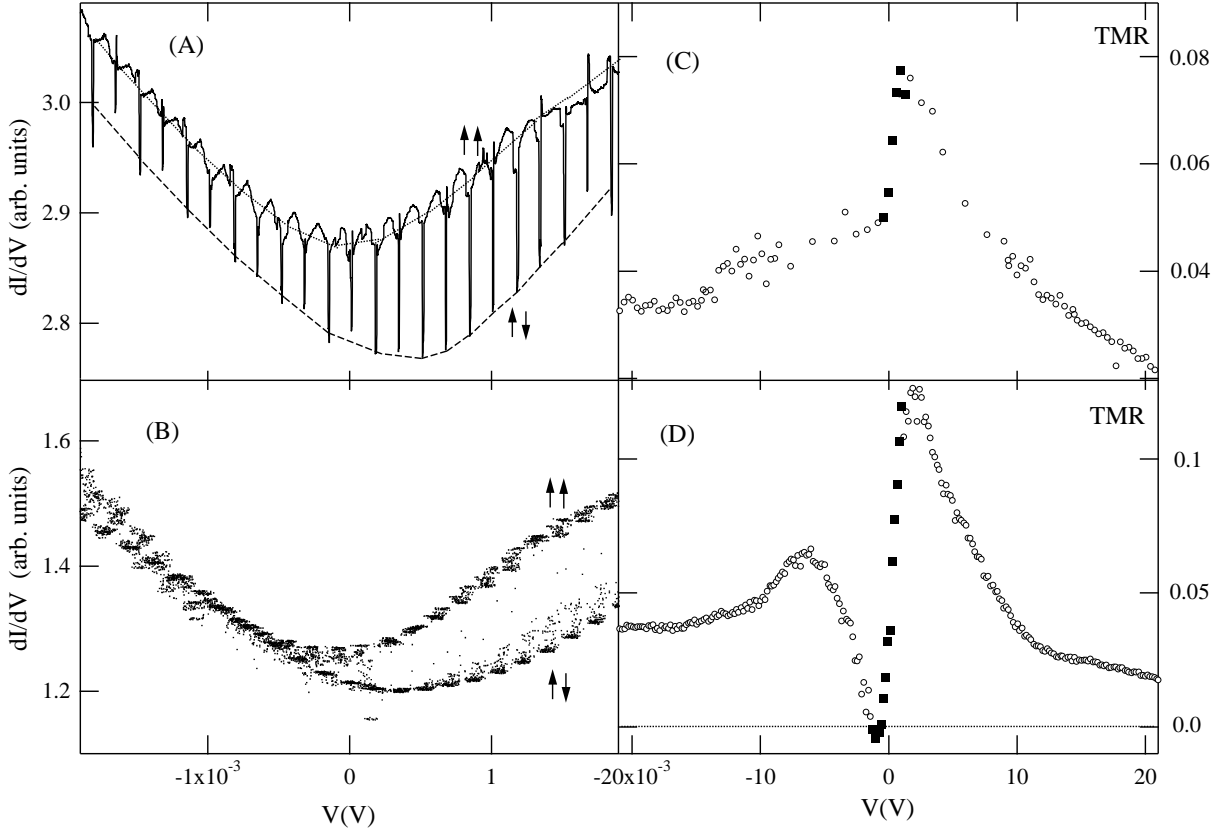


FIG. 3: A and B: Differential conductance versus bias voltage in samples 1 and 2, respectively. C and D: TMR versus bias voltage in samples 1 and 2, respectively.

Assuming that grains are ballistic, we find $\tau_{e-ph}(eV) = 0.6ns$ at $V = 6mV$. As discussed above, $\tau_L \sim T_2$ because P is large. It follows that the injected electrons relax to the ground state much faster than they escape from the grains, because the Elliot-Yafet relation in Al implies $T_2 \gg \tau_{e-ph}(eV)$. So, the distribution of electrons in the grain is in equilibrium.

In the antiparallel state, electron spins accumulate in the grains by transport. If T_2 is much longer than the dwell time, spin accumulation creates a difference PeV between the Fermi levels of spin up and spin down electrons, as shown in Fig. 4-B. If T_2 is comparable to the dwell time, spin-up electrons in energy window $[E_F - PeV/2, E_F + PeV/2]$ can undergo a transition into one of the unoccupied spin-down states at lower energies, as sketched by the arrow. So, TMR decreases with V because electron-phonon transition time τ_{e-ph} decreases with V , thereby causing T_2 to decrease with V , because $T_2 = \tau_{e-ph}/\alpha$.

First, we estimate T_2 at zero bias voltage. Typical excitation energy at 4.2K is $\omega \approx$

$3.5k_B T = 1.3meV$. Eq. 2 gives the average transition time $\tau_{e-ph} = 60ns$ between the excited states at 4.2K and $T_2 = \tau_{e-ph}/\alpha = 0.6ms$.

Next, we estimate the characteristic voltage for *TMR* and compare it with data. T_2 begins to decrease with V when the spin-flip transition probability in energy window $[E_F - PeV/2, E_F + PeV/2]$ begins to increase with V . T_2 -reduction is significant when the difference between the highest occupied spin-up state and the lowest empty spin-down state is of order thermal energy, roughly when PeV is comparable to the Fermi distribution width $3.5k_B T$. So, the characteristic voltage is $3.5k_B T/(Pe)$. We obtain the characteristic voltage of 6.5mV and 5.4mV in samples 1 and 2, respectively, in agreement with data.

In sample 2, $TMR > 0$ at large negative bias, even though electron transport at $V \sim -1mV$ is unpolarized. This behavior can be explained by the distribution of charging energies among grains. At large bias, smaller grains contribute more significantly to the conductance, because smaller grains have larger charging energy and require more voltage to pass current. Smaller grains also have larger level spacing. If the level spacing exceeds $k_B T$, the spin-relaxation process described above will freeze, leading to much longer T_2 and finite *TMR* at large bias.

Next, we discuss measurements of the Hanle effect. We apply a weak magnetic field B_n perpendicular to the magnetization direction. Consequently, the injected spins precess around the magnetic field with a Larmour period. When the Larmour period is larger than the dwell time, the spin-polarization of the current will be reduced to zero. Thus, one would naively expect that current versus B_n would exhibit a peak, and the peak width would be related to dwell time, which could then be used to measure T_2 directly.

Fig. 4-A displays current versus perpendicular field in sample 3 in the parallel configuration. The dependence is reversible when magnetic field is swept up and down, showing that the curve does not arise from the hysteresis loop in the leads. The amplitude of the peak in the figure is approximately the same as $(I_{\uparrow\uparrow} - I_{\uparrow\downarrow})/2$, showing that spin-polarization of the current is reduced to zero. The characteristic field, defined as half-width of the peak, is 8mT. The corresponding spin-precession period is $h/2\mu_B B_n = 4.4ns$. The naive picture would suggest the dwell time of order ns .

But, we find that the half-width is not asymmetric with bias voltage, even though *TMR* is strongly asymmetric. We have confirmed this behavior in another sample, where the half-width was $2mT$. This suggests that the half-width in Fig. 4-A is unrelated to dwell

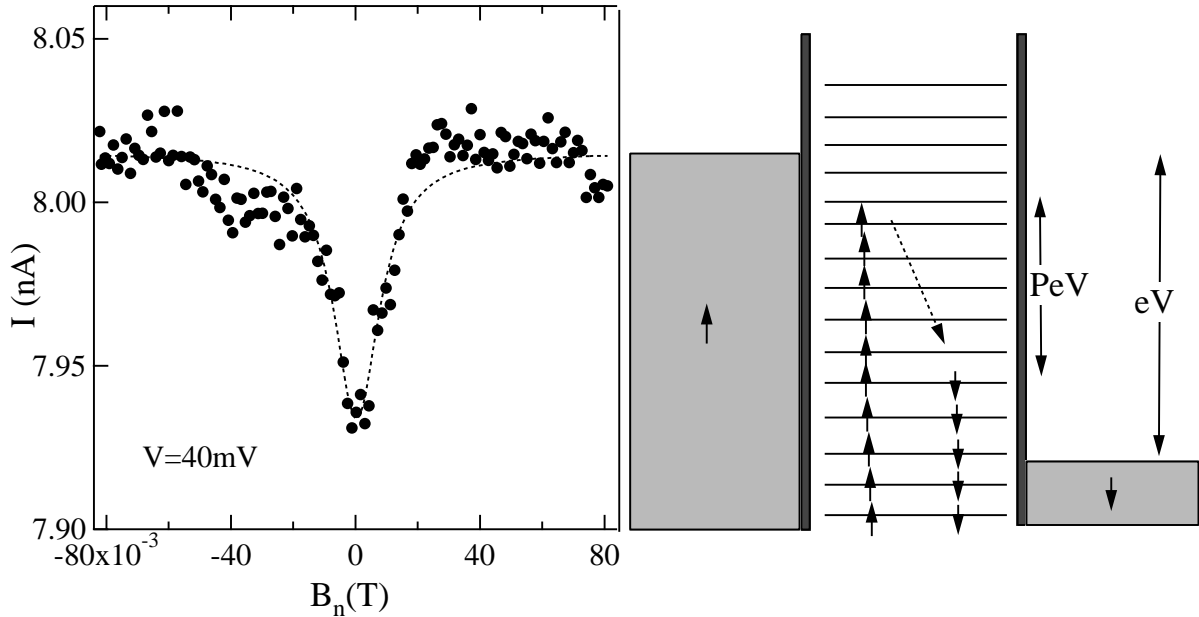


FIG. 4: A. Current versus perpendicular field in sample 3. B. Sketch of the grain electronic configuration at bias voltage V . The arrow indicates electron-phonon induced transition with spin-flip.

time.

We propose that I versus B_n describes the statistical distribution of local fields in the ensemble. The local field could be generated by the magnetization of the reservoirs. Surface roughness, for example, can create a finite dipole field. Injected spins then precess around the local field at the Larmor frequency. In the presence of local field, TMR is finite because the component of the injected spin along the local field direction is constant. This component is responsible for spin-polarized current.

The injected spins become decoupled from the local field when the applied perpendicular field exceeds the average local field. In a strong perpendicular field, spins precess perpendicular to the magnetization direction and the spin-polarized current is zero. Thus, Fig. 4-A displays the local-field distribution in the ensemble of grains. The average local field of 8mT is reasonable, because the internal field in Co (2T) is much larger than 8mT.

In conclusion, we study spin-polarized current through ensembles of nm-scale Al grains connected in parallel. Tunnelling magnetoresistance demonstrates that electron transport is spin coherent in one current direction and incoherent in the other current direction.

This behavior is attributed to asymmetry in electron dwell times and spin-decoherence. The tunnelling magnetoresistance decreases rapidly with bias voltage, suggesting that spin-decoherence time scales with electron-phonon transition time. We apply the Elliot-Yafet relation and estimate spin-coherence time of $T_2 \approx 0.6ms$ at 4.2K, which is extremely long and suggests that quantum computation with spins at 4.2K could be feasible.

This work was performed in part at the Georgia-Tech electron microscopy facility. This research is supported by the David and Lucile Packard Foundation grant 2000-13874 and Nanoscience/Nanoengineering Research Program at Georgia-Tech.

-
- [1] G. A. Prinz, *Science* **282**, 1660 (1998).
 - [2] S. A. Wolf, D. D. Awschalom, R. A. Buhrman, J. M. Daughton, S. von Molnar, M. L. Roukes, A. Y. Chtchelkanova, and D. M. Treger, *Science* **294**, 1488 (2001).
 - [3] D. D. Awschalom, D. Loss, and N. Samarth, *Semiconductor Spintronics and Quantum Computation* (Springer Verlag, 2002).
 - [4] D. Loss and D. P. DiVincenzo, *Phys. Rev. A* **57**, 120 (1998).
 - [5] G. Burkard, H. A. Engel, and D. Loss, *Fortschr. Phys.* **48**, 965 (2000).
 - [6] J. M. Kikkawa, I. P. Smorchkova, N. Samarth, and D. D. Awschalom, *Science* **277**, 1284 (1997).
 - [7] T. Fujisawa, D. G. Austing, Y. Tokura, Y. Hirayama, and S. Tarucha, *Nature* **419**, 278 (2002).
 - [8] J. M. Elzerman, R. Hanson, L. H. W. van Beveren, B. Witkamp, L. M. K. Vandersypen, and L. P. Kouwenhoven, *Nature* **430**, 6998 (2004).
 - [9] V. N. Golovach, A. Khaetskii, and D. Loss, *Phys. Rev. Lett.* **93**, 016601 (2004).
 - [10] M. Johnson and R. H. Silsbee, *Phys. Rev. Lett.* **55**, 1790 (1985).
 - [11] E. I. Rashba, *Phys. Rev. B* **62**, R16267 (2000).
 - [12] R. J. Elliot, *Phys. Rev.* **96**, 266 (1954).
 - [13] H. R. Zeller and I. Giaver, *Phys. Rev.* **181**, 789 (1969).
 - [14] D. V. Averin and K. K. Likharev, in *Mesoscopic Phenomena in Solids*, edited by B. L. Altshuler, P. L. Lee, and R. A. Webb (Elsevier and Amsterdam, 1991), p. 169.
 - [15] C. T. Black, D. C. Ralph, and M. Tinkham, *Phys. Rev. Lett.* **76**, 688 (1996).
 - [16] M. Julliere, *Phys. Lett. A* **54**, 225 (1975).

- [17] S. O. Valenzuela, D. J. Monsma, C. M. Marcus, V. Narayanamurti, and M. Tinkham, cond-mat/0407489 (????).
- [18] F. J. Jedema, M. S. Nijboer, A. T. Filip, and B. J. van Wees, Phys. Rev. B **67**, 085319 (2003).
- [19] O. Agam, N. S. Wingreen, B. L. Altshuler, D. C. Ralph, and M. Tinkham, Phys. Rev. Lett. **78**, 1956 (1997).
- [20] The IV-curve of an ensemble of grains does not have a gap at $V = 0$, so, the dwell times change in voltage interval $\sim k_B T/e$ around zero bias, not E_C/e .